Australian Journal of Basic and Applied Sciences, 4(3): 457-467, 2010
ISSN 1991-8178

Soil Surface Salinity Prediction Using ASTER Data: Comparing Statistical and Geostatistical Models

[1]Toktam Tajgardan, [2]Shamsollah Ayoubi, [3]Shaban Shataee, [4]Kanwar L. Sahrawat

[1]Department of Soil Science, College of Agriculture, Gorgan University of Agricultural Science and Natural Resources, Gorgan, Iran.
[2]Department of Soil Science, College of Agriculture, Isfahan University of Technology, Isfahan, 84156-83111, Iran
[3]Department of Forestry, Gorgan University of Agricultural Science and Natural Resources, Gorgan, Iran.
[4]International Crop Research Institute for the Semi Arid Tropic (ICRISAT), Patancheru, 502 324, Andhra Pradesh, India.

Abstract: This study was conducted to evaluate the performance of univariate spatial (ordinary kriging- OK), hybrid/multivariate geostatistical methods (regression-kriging- RK, Co-kriging- CK) with multivariate linear regression (MLR) in incorporation with ASTER data in order to predict the spatial variability of surface soil salinity in an arid area in northern Iran. The primary attributes were obtained from grid soil sampling with nested-systematic pattern of 169 samples and the secondary information extracted from spectral data of ASTER satellite images. The principal component analysis, NDVI and some suitable ratioing bands were applied to generate new arithmetic bands. According to validation based RMSE and ME calculated by a validation data set, the predictions for soil salinity were found to be the best and varied in the following order: $RK_{ASTER\text{multivariate}} > REG_{ASTER\text{multivariate}} > Co\text{-}kriging_{ASTER} > kriging$. Overall, this comparative study demonstrated that RK approach was a better predicator than other selected methods to predict spatial variability of soil salinity. The overall results confirmed that using ancillary variables such as remotely sensed data, the accuracy of spatial prediction can further improved.

Key words: Aster, electrical conductivity, geostatistics, spatial prediction.

INTRODUCTION

Salinization is one of the main causes of soil degradation in arid and semi-arid regions around the world. It reduces plant growth, agricultural production, and increases soil erosion and the reclamation of such land resources is expensive and at times beyond the means of poor farmers (Fernandez-Buces *et al.,* 2006; Szabolcsm, 1989). Saline lands are sensitive to changes in climate, soil and hydrological properties in time and space (Fernandez-Buces *et al.,* 2006; Kerte sz and To th, 1994). The characterization and mapping of soil salinity is difficult because of high seasonal and spatial variability in salt concentration (Fernandez-Buces *et al.,* 2006).

The global extent of primary salt-affected soils is about 955 Mha, while the secondary salinization affects some 77 Mha, with 58% of these in irrigated areas (Metternicht *et al.,* 2003). The salt-affected soils are usually characterized considering soil water content, depth, evaporation, rainfall, chemical and physical properties such as pH, ECe, ESP, Na^+ and other anion and cations (Fernandez-Buces *et al.,* 2006; Kerte sz and To th, 1994). To create thematic maps using conventional mapping technique requires analyses of a large number of samples using an extensive plan, resulting in high investment of time and cost. Besides, investigation and basic management need to be timely based on the quantitative information accessed using field spectroscopy and remote sensing (Milton, 1987).

Reflectance is a property, which is derived from the inherent spectral behavior. In earth surface studies, spectral values of satellite images are closely related with soil surface physical and chemical characteristics, especially salinity (Fernandez-Buces *et al.,* 2006). This relationship is commonly studied using linear regression

Corresponding Author: Toktam Tajgardan, Department of Soil Science, College of Agriculture, Gorgan University of Agricultural Science and Natural Resources, Gorgan, Iran.
E-mail: tajgardan_toktam@yahoo.com
Fax: +98-311-3913471 , Tel: +98-311-3913470

method. Therefore, digital information in different spectral bands can be used in the measurement of related soil characteristics (Goulard and Voltz, 1992; Van der Meer, 2000). Several authors have characterized salt-affected soils using satellite images, airborne photos and land radiometric techniques, based on the correlation studies between spectral reflectance by salt content and soil salinity/alkalinity indicators to generate soil salt spatial distribution map (Csillag *et al.,* 1993; Fernandez-Buces *et al.,* 2006; Verma *et al.,* 1994).

Spatial analysis, interpolation and producing the maps of soil properties can be obtained by different techniques, such as ordinary kriging (Lopez-Granados *et al.,* 2002; Paz-Gonzalez *et al.,* 2000) cokriging (Rivero *et al.,* 2007; Websrer and Oliver, 2001), kriging-regression (Lopez-Granados *et al.,* 2005; Odeh *et al.,* 1995). A numerous number of studies have been made for salinity prediction using geostatistical techniques (Hajrasuliha *et al.,* 1980; Hosseini *et al.,* 1994; Odeh *et al.,* 1995; Walter *et al.,* 2001). Geostatistical prediction methods have opened up the possibility of mapping soil properties by using auxiliary data and cross-variogram, which require about 100 sampling points (Kerry and Oliver, 2003). The prediction methods that incorporate secondary informative variable with high spatial correlation, according to the target variable, such as digital numbers of satellite image or digital elevation model (DEM), have been developed for use on a larger scale, reducing time and costs.

Considerable researches have been conducted on the use of statistical and geostatistical techniques for the mapping of soil properties using series of satellite data such as bare soil landsat TM (thematic mapper) imagery and AVHRR (advanced very high resolution radiometer) data from the NOAA (national oceanic and atmospheric administration (Bishop *et al.,* 2001; Kerte sz and To th, 19994) landsat ETM$^+$ (Enhanced thematic mapper plus) and ASTER (Advanced space borne thermal emission and reflection radiometer) for soil phosphorus variability (Rivero *et al.,* 2007) and SPOT2 satellite (Douaoui *et al.,* 2006) for detecting the salinity hazards.

No attempt however, has been made to incorporate ASTER data in the geostatistical approach for soil salinity mapping in the arid regions. Therefore, this study was conducted to delineate soil salinity areas based on an intensive and regular soil sampling, and using different prediction methods for arriving at the best approach for soil salinity mapping in the sample area in Golestan province of Iran.

MATERIALS AND METHODS

Description of the Study Area:

The study area located in north western of Iran, Golestan province in 25 km of Aq Qala town between 37° 12′ 18″ and 37°13′ 32″ northern latitudes and 54° 22′ 18″ to 54° 29′ 1″ eastern longitudes (Fig 1), which covers 2000 ha area. The mean annual precipitation is 230.5 mm, which falls mainly from November to March. The mean annual temperature is 19.01°C. According to the previous study (Akbarlo, 1995), the climate of the area is a temperate semiarid. The study area is flat (maximum slope of 2%) and in some parts has loessial hills. According to Soil Taxonomy (Soil Survey Staff, 2006), the soils of the study area are dominantly classified as:

Fine-loamy, mixed, superactive, calcareous, thermic, Gypsic Aquisalids

Data:

The spatial soil salinity data used in this study was obtained using an intensive grid soil sampling. A selected area of 2000 ha was sampled with intervals of 50, 100, 250, 500, 1000 m, in 169 sampled points on a nested regular pattern (Fig 2). Soil samples (0-5 cm) were collected on middle of July 2006. The position of each point was registered with GPS. Soil samples were air-dried and passed through 2 mm sieve for EC_e measurement. The surface electric conductivity (EC_e) was measured using conductimeter (Inolab720.wtw) in saturated soil extract (Page *et al.,* 1992). In this study the VNIR and SWIR bands of ASTER from 2006 year were used. The table 1 shows the description of VNIR and SWIR bands.

Geometric Correction and Image Processing:

The VNIR and SWIR bands were georefrenced with an available orthorectifed ETM$^+$ 2002 imagery using image to image registration method and were rectified to the UTM zone 40 cartographic projections. Nearest neighbor re-sampling type was used with the absolute field location accuracy (30 m, 15 m). The remote satellite images were processed using the Geomatica V.8.0.1 software. In addition to main bands, some suitable processing operations including, first component from selective principal component analysis of VNIR bands and SWIR bands and standard principal component analysis of VNIR and SWIR data (Ren and Abdelsam, 2006), the NDVI (Normalized Difference Vegetation Index) from VNIR bands (Rouse *et al.,* 1974) and some ratio arithmetic bands were applied to identify salinity quantification (Table 2).

Extraction of Spectral Number of Sample Points:

The spectral numbers (DN) of each sample point on main and proccessed bands were extraced using extract function in IDRISI software. These spectral numbers were used for statistical analysis.

Statistical and Geostatistical Prediction Analysis:

Multiple Linear Regression (MLR) Method:

Every sampled soil point was located in the original images and synthetic images were extracted. It was verified that all spectral values were normally distributed. Pearson linear correlations were determined between ECe and spectral values in all bands, accepting a confidence level of 95%. Regression equation was developed for those variables that showed higher significant correlation with digital numbers. The statistical analysis was performed using SPSS statistical package (SPSS v. 13.0). Regression analysis was performed using following equation:

$$Z^*_{(SR)}(S_0) = f[RSInd(S_0)] \quad (1)$$

Where *RSInd* the index is derived from the remote sensing data observed at S_o and *f* is the regression function (Douaoui *et al.,* 2006). Spatial distribution of ECe was constructed applying this equation to the images.

Geostatistical Analysis:

Spatial variation with interdependence is commonly described with a variogram (Warrik *et al.,* 1989). In geostatistics, the concept of variance from classic statistics is extended to semivariance. The spatial structure of each property was characterized by experimental semivariogram using the following equation (Lopez-Granados *et al.,* 2005):

$$\gamma_h = \frac{1}{N}\sum_{i=1}^{N(h)}[z(x_i+h)-z(x_i)]^2 \quad (2)$$

where γ_h is the experimental semivariogram value at distance interval h; N(h): number of sample pairs within distance interval h; z(xi), z(xi+h): sample values at two points separated by the distance interval h. Spherical, exponential models were fitted to the experimental semivariograms defined by Eqs. (3) and (4) respectively (Deutsch and Journel, 1998):

$$\gamma_h = C_o + C[1.5(h/a)-0.5(h/a)^3], \qquad \text{If } h \le a \quad (3)$$

$$\gamma_h = C_o + C \qquad \text{If } h > a$$

$$\gamma_h = C_o + C[1-\exp(-3h/a)] \quad (4)$$

where a is the range, C_o the nugget effect, and C_o+C the sill or total semivariance.

Ordinary kriging (OK):

This method solely utilizes primary data as ECe measured at sampled locations u_a to estimate ECe at unsampled locations. The constancy of the mean is assumed only within a local neighborhood *W(u)* centered at the location u being estimated. Here, the mean is deemed to be a constant but unknown value, i.e., m(u')=constant but unknown, u'εW(u). The OK estimator is written as a linear combination of the n(u) data $Z(u_a)$ with a single biasedness constraint (Simbahan *et al.,* 2006):

$$Z^*_{OK}(u) = \sum_{\alpha=1}^{n(u)} \lambda_\alpha^{OK}(u) Z(u_\alpha), \qquad \text{With} \quad \sum_{\alpha=1}^{n(u)} \lambda_\alpha^{OK} = 1 \quad (5)$$

In addition to OK, we evaluated RK and Co-kriging as hybrid interpolation methods in which soil variation is quantified using deterministic and empirical models incorporate one or more ancillary variables in the estimation of ECe.

Regression-kriging (RK):

This method is based on the use of simple or multiple regressions with simple kriging (Lark and Beckett, 1995; Odeh *et al.,* 1995) for the investigation of spatial variability of continuous variables. This kriging method is an interpolation that incorporates secondary information into the kriging system (Lopez-Granados *et al.,* 2005). The method uses the auxiliary variables (spectral data) to define the spatial trend of the target variable (ECe) and performs simple kriging on the residuals (Goovaerts, 1997). Therefore, after applying the multiple linear regression models to image data from ASTER in the given points, the residual values were extracted. At each sampling point, the residual value was calculated by subtracting the trend estimate (multiple linear functions) from the original ECe value. Then, the appropriate semivariogram was fitted to residuals and simple kriging was carried out on the residuals. The final estimate of ECe was obtained by adding the trend estimate to the simple kriged estimate of the residuals (Goovaerts, 1997; Odeh *et al.,* 1995). The step by step flow chart of this method is presented in Fig 3.

Cokriging (CK):

Cokriging is a multivariate extension of kriging in which the secondary information is incorporated in the estimation at unsampled locations by accounting for multi-scale correlations of the primary variable Z_1 and N_v-1 secondary attributes Z_v (Dobermann *et al.,* 1997; Goovaerts and Webster, 1994). Auto and cross-variograms of all primary and secondary variables were computed and modeled in the form of a linear model of coregionalization (Gulard and Voltz, 1992). The co-located CK estimator for an unsampled location u is then:

$$Z_{COK}^{*}(u) = \sum_{\alpha=1}^{n(u)} \lambda_{\alpha}(u)[Z_1(u_{\alpha})] + \sum_{v=2}^{N} \lambda_v(u)[Z_v(u) - m_v + m_1] \quad (6)$$

The statistical analysis was performed using SPSS statistical package (Wagner, 2007) and Minitab (Gardiner, 1997). Geostatistical analysis was performed using Variowin (Panattier, 1996) and GS^{+} software (GS^{+} v. 5.1) to fit the semivariograms, cross variogram, and kriging analysis.

Comparison of Estimation Methods:

The performance of the different interpolation methods was assessed by cross-validation (Issaks and Srivastava, 1989). The mean error (ME) and root mean square error (RMSE) were used to evaluate model performances in cross-validation mode.

Validation was performed using 36 samples randomly chosen from the 169 samples (approximately 20% of all samples). Indices were adopted for comparing four mapping methods including kriging, co-kriging, kriging-regression and multiple linear regression, in this, i.e.; mean error (ME) and root-mean-square-error (RMSE):

$$ME = \frac{1}{N}\sum_{1}^{N}[Z^{*}(x_i) - Z(x_i)] \quad (7)$$

$$RMSE = \sqrt{\frac{1}{N}\sum_{1}^{N}\left[Z^{*}(x_i) - Z(x_i)\right]^2} \quad (8)$$

where:

N; Number of validation points

$Z^{*}(x)$; estimated value at point x_i and $Z(x_i)$; ground observation value at point x_i.

RESULTS AND DISCUSSION

Descriptive statistical of EC_e in the selected area showed mean value and standard deviation, 105.93 and 59.57dS/m respectively. The coefficient of variation (CV) value of EC_e calculated 0.56. To define variability into categorical classes, we followed the system suggested by Wilding (Wilding, 1985). According to this classification any property with CV more than 0.35 is classified as high variable, therefore, EC_e indicated high variability in the selected area. Low skewness value (0.011) confirmed that the given property followed up the normal distribution in the study area.

Pearson linear correlations between digital numbers of Aster data and measured EC_e values (Table 3) revealed that EC_e showed significant correlations ($p<0.05$ and $p<0.01$) with spectral data in all of bands, except VNIR1 and VNIR2. Negative correlation meant that small digital numbers for all bands except SWIR5, NDVI, PCA3 bands corresponded to high values of EC_e.

Linear stepwise regression model was derived to predict EC_e using ancillary datasets (i.e., spectral data and indices) as predictor variables. The results showed the significant ASTER data ($P<0.05$) with ECe included *SWIR1, SWIR6, SUM48, PCA2,* and they contributed in the multiple regression model with the highest R^2.adj of 0.45, and the lowest Cp, MSEp, ME and RMSE. The regression model for prediction of EC_e and its statistics are summarized in Table 4. Khajeddin (Khajeddin, 1995) indicated that among MSS data, MSS1 and MSS2 data had highest correlation with EC_e. Douaoui *et al.* (Douaoui *et al.,* 2006) revealed that the salinity index (SI3= $\sqrt{G^2 + R^2}$) synthesized by SPOT data, showed the highest correlation(r= 0.49) with soil salinity.

The experimental variogram was obtained for soil surface EC_e (Fig 4a). An exponential model was fitted to the experimental variogram with a nugget effect of 2278.62 $(dS/m)^2$, a sill of 1935.73 $(dS/m)^2$ and a range of 4700 m (Table 5). Range is the distance beyond which spatial dependence between soil samples is ceases to exist and it can be used as indicator of the appropriate cell size for a filed survey in site-specific management (Lopez-Granados *et al.,* 2005). Thus, range is important, both to define the different classes of spatial dependence for the soil variables as described previously in Lopez-Granados *et al.*, (2005) and to establish the sampling interest for future surveys. The sampling interval should be less than half of the range as a "rule of thumb" (Kerry and Oliver, 2003). The ratio of dependency ($C_o/C+C_0*100$) for EC_e, calculated 54%. Different classes of spatial dependency for the soil variable can be evaluated by the described ratio [3]. For the ratio between 26 and 75%, the soil variable was considered to be moderately spatially dependent. Therefore, in the study area soil surface salinity showed moderately spatial dependency.

The co-kriging (CK) is the logical extension of kriging to situations where two or more variables are spatially independent, and one of them, the one of immediate interest, is undersampled (McBratney and Webster, 1983). Pearson linear correlation between soil EC_e and spectral values of ASTER bands (Table 4) revealed that SWIR1 showed highest correlation with EC_e data, although this correlation was moderate (r=0.43), but it was used as auxiliary variable in this method.

To investigate spatial variability structure of EC_e and SWIR1 spectral band, experimental variograms were calculated for those variables in different directions (0˚, 45˚, 90˚ and 135˚). After of confidence of isotropy in all selected direction, omnidirectional variogram was considered for subsequent analysis. Theoretical variograms were fitted to EC_e and SWIR1 data respectively with calculated models in Figs 4a and 4b. The illustration of interrelationships of two variables is presented in Fig 4c.

As already explained, for bi-variate interpolation method, the SWIR1 data was used as an exhaustive secondary information source. Therefore in order to co-kriging analysis was necessary to calculate cross-variogram of EC_e and SWIR1 band data. Since soil electrical conductivity was negatively correlated with SWIR1 band data, therefore the cross semi-variogram was negative (Fig 4c). Table 5 shows the coregionalization parameters for EC_e with the fitted models. Rivero *et al.* (2007) showed for prediction soil phosphorus variability in a Florida wetland with ASTER and ETM^+ data, the NDVI index had strongest spatial cross-semivariogram structure for soil TP and a spherical model was fitted for prediction of TP with this method (CK).

The experimental variogram was calculated for the residual value of EC_e estimated use of multiple regression model (REGm) (Fig 5). An spherical model was fitted to the experimental variogram with a nugget effect of 1530.5 $(dS/m)^2$, a sill of 1519.58 $(dS/m)^2$ and a range of 1226.5 m (Table 5).

For comparing results of different predictors, correlation coefficient (r), ME and RMSE determination were used of 20% data (n=36) to evaluate the performance of the map prediction quality. Validation results for ECe prediction from the four geostatistical and statistical methods are summarized in Table 6 including ordinary kriging (OK), co-kriging (CK), regression kriging model based on the multivariate regression model (RK) and linear regression model.

ME and RMSE value calculated for different approaches (Table 6) showed that higher predictions errors were obtained with kriging and cokriging methods. Regression-kriging (RK) approach was clearly the best method for the prediction of ECe showing the lowest ME (-1.04) and RMSE (44.08) values and highest correlation coefficient (0.66). According to validation based RMSE and ME calculated by a validation data set, the predictions for soil salinity were found to be the best and varied in the following order:
$RK_{ASTER\text{mutivariate}} > REG_{ASTER\text{multivariate}} > Co\text{-}kriging_{ASTER} > Kriging$. Therefore, the map derived using RK method could be used as the best qualified map for salinity management in the given study area.

Douaoui *et al.*(2006) in detecting salinity hazards within a semiarid context by means of combining soil and ETM^+ data found that RK performed better than other spatial models including multiple linear regression (MLR), ordinary kriging (OK), classification method (CL), and classification-kriging. In another study,

Rivero *et al*. (2007) recommended the ETM-NDVI (model REGETM) showed a stronger relationship to soil phosphorus (r =0.68) to predict soil phosphorus variability with RK rather than other interpolation methods. Odeh and McBratney (2000) demonstrated superiority of RK to other prediction methods such as OK, universal kriging, multiple-linear regression and CK. Dungan (1998) in comparing geostatistical (OK, CK and stochastic simulation) with linear regression for prediction vegetation parameters indicated that correlation coefficients between main and secondary data more than 0.89, the best model was obtained for CK. Knotters *et al*. (1995) showed that correlation coefficients more than 0.70, CK and kriging combined with linear regression methods produced better results. Ordinary kriging method, showed the poorest prediction results, because of the spectral data was ignored and only the measured EC values were considered. Therefore when secondary information is available, was suggested to incorporate them into soil properties for providing map.

Fig. 1: Location of the study area in the Golestan province, northern Iran

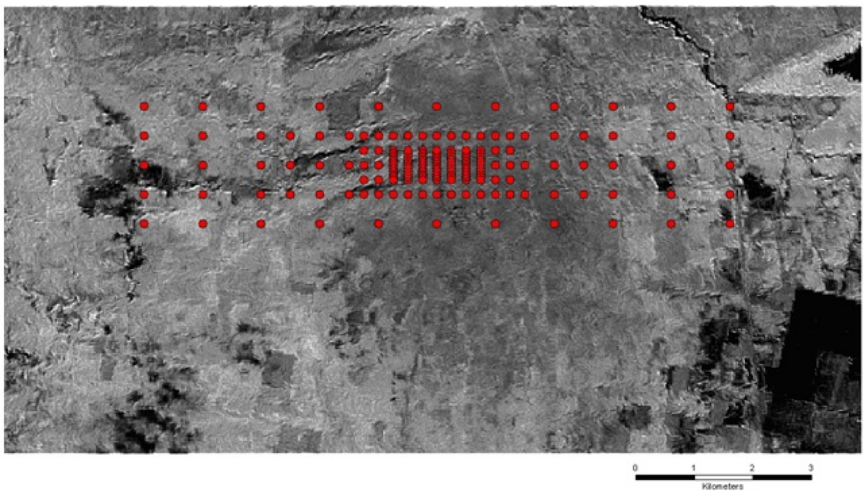

Fig. 2: Soil sampling grid on the ASTER image (SWIR1 band)

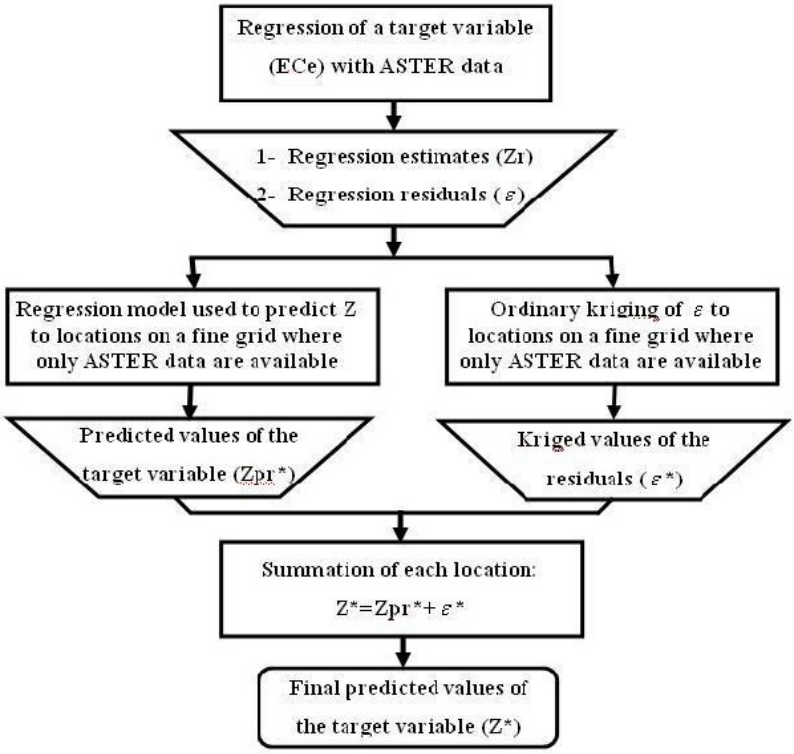

Fig. 3: Flow chart of regression-kriging method (Odeh *et al.,* 1995)

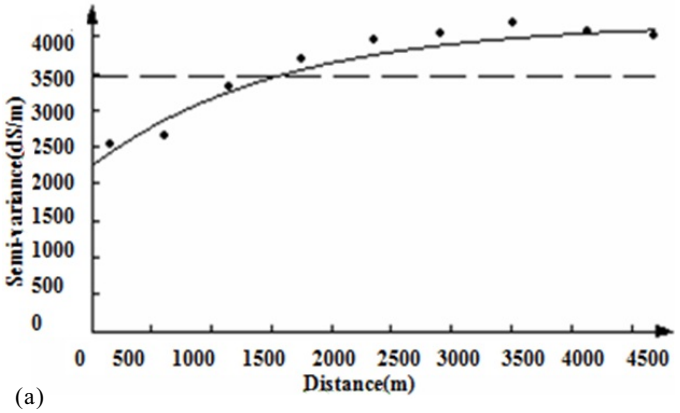

(a)

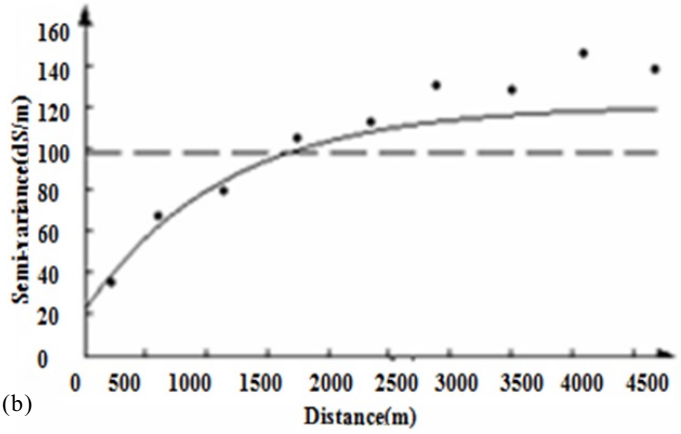

(b)

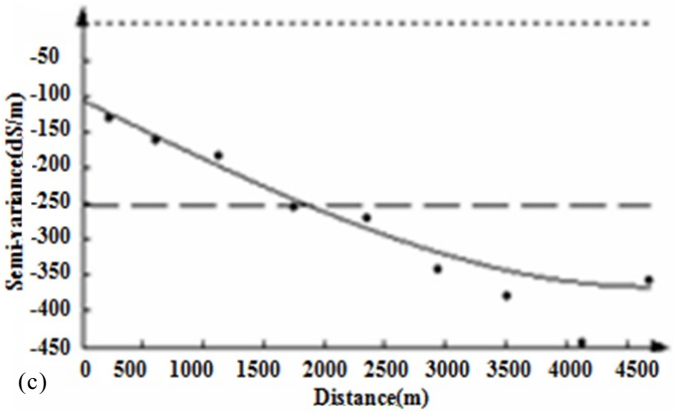

Fig. 4: Experimental variograms and fitted variograms for ECe and spectral band: a) ECe surface b) SWIR1 spectral band c) Cross variogram ECe-SWIR1 band.

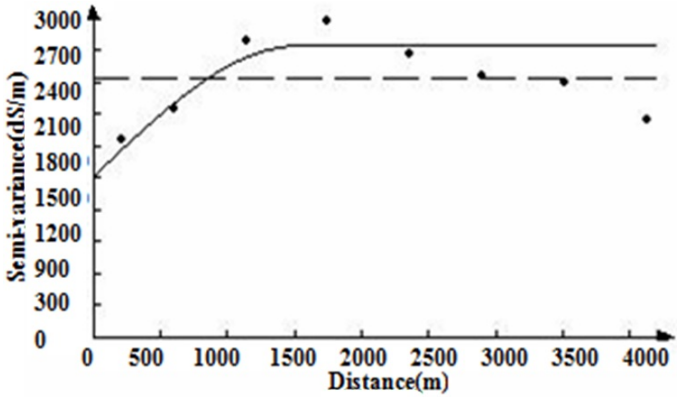

Fig. 5: Experimental and fitted variogram for ECe residuals (REGm)

Table 1: The description of VNIR and SWIR bands of ASTER data

Subsystem	Band No.	Spectral range (μm)	Spatial resolution (m)	Quantization levels
VNIR	1	0.52-0.6		
	2	0.63-0.69	15	8 bits
	3N	0.78-0.86		
	3B	0.78-0.86		
SWIR	4	1.60-1.70		
	5	2.145-2.185		
	6	2.185-2.225	30	8 bits
	7	2.235-2.285		
	8	2.295-2.365		
	9	2.360-2.430		
TIR	10	8.125-8.475		
	11	8.475-8.825		
	12	8.925-9.275	90	12 bits
	13	10.25-10.95		
	14	10.95-11.65		

Table 2: Main and processed bands

Bands	(bands made procedure)	No.
*VNIR*1.....*SWRI*6	Main bands of ASTER except TIR bands	1
PCA1vnir	First component of PCA of VNIR bands	2
PCA1swir	First component of PCA of SWIR bands	3
PCA1vnir&swir*	First component of PCA of VNIR&SWIR bands	4
NDVI**	(*vnir* 3-*vnir* 2)/(*vnir* 3+*vnir* 2)	5
SUB48	(*swiir*1/*swir*5)	7
SUM48	(*swiir*1+*swir*5)	8

*(Ren and Abdelsalm, 2006)

**: (Jimenez-Munoz *et al.,* 2006; Rouse *et al.,* 1974)

Table 3: Correlation coefficients between spectral indices and measured EC_e values

Spectral bands	Correlation coefficients (EC_e)
SWIR1	-0.433**
SWIR2	-0.344**
SWIR3	-0.366**
SWIR4	-0.316**
SWIR5	0.287**
SWIR6	-0.361**
VNIR1	-0.046
VNIR2	-0.093
VNIR3	-0.185*
NDVI	0.177*
PCA1vnir	-0.314**
PCA1swir	-0.241**
PCA1vnir&swir*	0.315**
SUM48	-0.373**
SUB48	-0.276***

Correlation is significant at the 0.01 level. * Correlation is significant at the 0.05 level

Table 4: Regression model to predict ECe with spectral values

Model	R	R^2.adj	Cp	MSEp	RMSE	ME
ECe = 730-12.4Swir1-9.77Swir6+15.5 sum48-1.64 PCA1swir	0.68	0.45	0.037	0.41	52.24	-0.60

Table 5: Geostatistical analysis of electric conductivity (EC_e), spectral band(SWIR1), coregionalization matrix parameters (CK) and regression kriging (RK)

Prediction model	Variogram model	Sill	Nugget	Range (m)
Ordinary kriging (OK)	Exponential	1935.73	2278.62	4700
SWIR1	Exponential	98	23.52	3429.75
Ec_e-SWIR1	Spherical	-260	-109.55	4700
RK(kriging of residuals)	Spherical	1519.58	1530.5	1226.5

Table 6: Summary of validation statistics ME and RMSE using of 20 % data (n=36)

Soil parameter	model	Correlation coefficient	ME	RMSE
EC_e	Regression-kriging	0.66	-1.04	44.08
	Multiple linear regression	0.55	-1.17	49.39
	Co-kriging	0.34	-1.60	59.42
	Ordinary kriging	0.33	-3.63	80.22

In general, geostatistical estimation methods incorporated to spectral data of ASTER had higher favorable RMSE results than multivariate regression prediction method using SWIR1, SWIR6, SUM48 and PCA1swir images derived from ASTER data. It seems that using only from one auxiliary variable such as SWIR1 with relatively low to moderate correlation coefficient with ECe, in CK technique, can not improve prediction, whereas addition of more correlated images including, SWIR6, SUM48 and PCA1swir in RK and MLR techniques improved prediction accuracy. These results are accordance with other studies (Knotter *et al.,* 1995; Odeh and McBratney, 2000; Rivero *et al.,* 2007). On the other hand ordinary kriging also showed lower accuracy than multiple linear regression combined with ASTER data, indicating that in ordinary kriging only the spatial component of soil variable was considered and the spectral data were completely ignored.

Conclusion:

Generally, results from this study confirmed that remote sensing data can play an important role in improving predictions of salinity levels, can be captured by these sensors. Depending on the strength of the relationships between target soil variable and ancillary environmental variables, the spatial variability of soil observations models differ in performance. Therefore, this comparative study in an arid zone showed, RK and multiple regression models could predict the soil surface salinity with more accuracy than other geostatistical and hybrid methods. Daytime ASTER data may show to what remote sensing improves salinity prediction models. The overall results exposed the using remote-sensing data and ground monitoring may be useful to map the soil salinity and manage them in the arid regions.

REFERENCES

Akbarlo, M., 1995. Vegetation analysis of saline and alkaline area in eastern mazandaran province, M. Sc., Gorgan University of Agricultural Sciences and Natural Resources, Goragn, Iran.

Bishop, T.F.A. and A.B. McBratney, 2001. A comparison of prediction methods for the creation of field-extent soil property maps. Geoderma, 103: 149-160.

Cambardella, C.A., T.B. Moorman, J.M. Novak, T.B. Parkin, D.L. Karlen, R.F. Turco and A.E. Konopka, 1994. Field-scale variability of soil properties in central Iowa soils. Soil Science Society of American Journal, 58: 1501- 1511.

Csillag, F., L. Pa´ stor and L.L. Biehl, 1993. Spectral band selection for the characterization of salinity status of soils. Remote Sensing of Environment, 43: 231-242.

Deutsch, C.V. and A.G. Journel, 1998. GSLIB. Geostatistical software library and users Guide, second ed. Oxford University Press, pp: 340.

Dobermann, A., P. Goovaerts and H. U. Neue, 1997. Scale dependent correlations among soil properties in two tropical lowland rice fields. Soil Science Society of American Journal, 61: 1483-496.

Douaoui, A.E.K., H. Nicolas, and C. Walter, 2006. Detecting salinity hazards within a semiarid context by means of combining soil and remote sensing data. Geoderma, 134: 217-230.

Dungan, J., 1998. Spatial prediction of vegetation quantities using ground and image data. International Journal of Remote Sensing, 19: 267-285.

Fernández-Buces, N., C. Siebe, S. Cram, J. L. Palasio, 2006. Mapping soil salinity using a combined spectral response index for bare soil and vegetation (a case study in the former lake Texcoco, Mexico), Journal of Arid Environments, 65: 644-667.

Gardiner, W.P., 1997. Statistics for the Biosciences: Data Analysis Using Minitab Software Science, 416.

Goovaerts, P., 1997. Geostatistics for Natural Resources Evaluation. Oxford University Press, New York.

Goovaerts, P., and R. Webster, 1994. Scale-dependent correlation between topsoil copper and cobalt concentrations in Scotland. European Journal of Soil Science, 45: 79-95.

Goulard, M. and M. Voltz, 1992. Linear coregionalization model: tools for estimation and choice of cross variogram matrix. Mathematical Geology, 24: 269-286.

Hajrasuliha, S., N. Baniabbasi, J. Metthey and D.R. Nielson, 1980. Spatial variability of soil sampling for salinity studies in southwest Iran. Irrigation Science, 1-12.

Hosseini, E., J. Gallichand and D. Marcotte, 1994. Theoretical and experimental performance of spatial interpolation methods for soil salinity analysis. Trans. ASAE,37(6): 1799-1807.

Issaks, E.H., R.M. Srivastava, 1989. An introduction to applied geostatistics. Oxford University Press.New York.

Jiménez-Muñoz, J.C., J.A. Sobrino, A. Gillespie, D. Sabol, and W. T. Gustafson, 2006. Improved land surface emissivities over agricultural areas using ASTER NDVI. Remote Sensing of Environment, 103: 474-487.

Kerry, R. and M. Oliver, 2003. Variograms of ancillary data to aid sampling for soil surveys. Precision Agriculture, 4: 261-278.

Kerte´ sz, M. and T. To´ th, 1994. Soil survey based on sampling scheme adjusted to local heterogeneity. Agroke´ mia e´ s Talajtan, 43(1-2): 113-132.

Khajeddin, S.J.A., 1995. Survey of the plant communities of Jazmorian Iran using landsat MSS data. Ph.D Thesis, University of Reading, UK.

Knotters, M., D.J. Brus and J.H.O. Voshaar, 1995. A comparison of kriging, cokriging and kriging combined with regression for spatial interpolation of horizon depth with censored observations. Geoderma, 67: 227-246.

Lark, R.M. and P.H.T. Beckett, 1995. A regular pattern in the relative areas soil profile classes and possible applications in reconnaissance soil survey. Geoderma, 68: 27-37.

Lopez-Granados, F., M. Jurado-Exposito, S. Atenciano, A. Garcia-Ferrer, M.S. De La Orden and L. Garcia-Torres, 2002. Spatial Variability of agricultural soil parameters in southern Spain. Plant and Soil, 246: 97-105.

Lopez-Granados, F., M. Jurado-Exposito, J.M. Pena-Barragan, L. Garcia-Torres, 2005. Using geostatistical and remote sensing approaches for mapping soil properties, European Journal of Agronomy, 23: 279-289.

McBratney, A.B. and R. Webster, 1983. Optimal interpolation and isarithmic mapping of soil properties V: Co-regionalization and multiple sampling strategy. Soil Science Society of American Journal, 34: 137-162.

Metternicht, G.I. and J.A. Zinck, 2003. Remote sensing of soil salinity: potentials and constraints. Remote Sensing of Environment, 85: 1-20.

Milton, E.J., 1987. Principles of field spectroscopy. International Journal of Remote Sensing, 8(12): 1807-1827.

Odeh, I.O.A. and A.B. McBratney, 2000. Using AVHRR images for spatial prediction of clay content in the lower Namoi Valley of eastern Australia, Geoderma, 97: 237-254.

Odeh, I.O.A., A.B. McBratney and D.J. Chittleborough, 1995. Further results on prediction of soil properties from terrain attributes. Hetrotropic co-Kriging and regression-kriging. Geoderma, 67: 215-226.

Page, A.L., R.H. Miller and D.R. Keeney, 1992. Method of soil analysis, chapter 15,19, 20 and 34, American Society of Agronomy Madison WL.USA.

Panattier, Y., 1996. VARIOWIN: Software for spatial data analysis in 2D, Springer-Verlag, New York.

Paz-Gonzalez, A., S.R. Vieira and M.T. Toboada Castro, 2000. The Effect of cultivation on the spatial variability of selected properties of an Umbric horizon. Geoderma, 97: 273-292.

Ren, D. and M. G.Abdelsalam, 2006. Tracing along-strike structural continuity in the Neoproterozoic Allaqi-Heiani Suture, southern Egypt using principal component analysis (PCA), fast Fourier transform (FFT),and redundant wavelet transform (RWT) of ASTER data. Journal of African Earth Sciences, 44: 181-195.

Rivero, R.G., S. Grunwald, and G.L. Bruland, 2007. Incorporation of spectral data into multivariate geostatistical models to map soil phosphorus variability in a Florida wetland. Geoderma, 140: 428-443.

Rouse, J.W., R.H. Haas, J.A. Schelle, D.W. Deering and J.C. Harlan, 1974. Monitoring the vernal advancement or retrogradation of natural vegetation. NASA/GSFC, Type III, Final report, Green-belt, MD, 371.

Simbahan, G.C., A. Achim Dobermann, P. Goovaerts, J. Ping and M. L. Haddix, 2006. Fine-resolution mapping of soil organic carbon based on multivariate secondary data.Geoderma, 132: 471-489.

Soil Survey Staff, 2006. Keys to Soil Taxonomy, USDA, NRCS, Washington.

Szabolcs, I., 1989. Salt-Affected Soils. CRC Press Inc., Boca Raton, FL 274pp.

Van der Meer, F., 2000. Geostatistical approaches for image classification and assessment of uncertainty in geologic processing. In: Advances in remote sensing and GIS analysis. P.M. Atkinson and N.J. Tate (Eds.), 147-166.

Verma, K.S., R.K. Saxena, A.K. Barthwal, and S.N. Deshmukh, 1994. Remote sensing technique for mapping salt affected soils. International Journal of Remote Sensing, 15(9): 1901-1914.

Wagner, W.E., 2007. Using SPSS for Social Statistics And Research Methods, Pine Forge Press, pp: 101.

Walter, C.,A.B. McBratney, A. Douaoui and B. Minasny, 2001. Spatial prediction of topsoil salinity in the Cheliff Valley, Algeria, using local ordinary kriging with local variograms versus whole-area variogram. Australian Journal of Soil Research, 39: 259-272.

Warrik, W., D.E. Myers and D.R. Nielson, 1989. Geostatistical methods applied to soil science, in: Page et al,(Eds.), Methods of Soil Analysis, Part 1, Physical and Mineralogical Method, Agronomy Monograph, No: 9: 53-81.

Webster, R. and M. Oliver, 2001. Local estimation or prediction: kriging. In: Geostatistics for Environmental Scientists. John Wiley and Sons, UK.

Wilding, L.P., 1985. Spatial variability: Its documentation, accommodation, and implication to soil surveys. In: D.R. Nielsen and J. Bouma (Eds.), Soil Spatial Variability. Pudoc. Wageningen, the Netherlands.